LA-UR- 04-2786

Approved for public release; distribution is unlimited.

Title: Equation of State and Neutrino Opacity of Dense Stellar Matter

Author(s): Sanjay Reddy, T-16

Submitted to: Proceedings First Argonne/MSU/JINA/INT RIA Workshop
The r-process: the astrophysical origin of the heavy elements and related Rare Isotope Acclerator Physics
(World Scientific)
I.N.T. Seattle, WA
January 8 - 10, 2004

Los Alamos
NATIONAL LABORATORY

EQUATION OF STATE AND NEUTRINO OPACITY OF DENSE STELLAR MATTER *

SANJAY REDDY
Theoretical Division
Los Alamos National Laboratory,
Los Alamos, NM 87545, USA
E-mail: reddy@lanl.gov

The properties of matter at densities similar to nuclear density plays an important role in core collapse supernova. In this talk I discuss aspects of the equation of state and weak interactions at high density. I highlight its relation to the temporal and spectral features of the neutrino emission from the newly born neutron star born in the aftermath of a core-collapse supernova. I will briefly comment on how this will impact r-process nucleosynthesis.

1. Introduction

The hot and dense neutron star (proto-neutron star) born in the aftermath of a core collapse supernova provides a promising environment for r-process nucleosynthesis. The intense temperatures and neutrino fluxes in the vicinity of the proto-neutron star is expected to result in a high entropy neutron-rich wind necessary for successful r-process nucleosynthesis. Although theoretical efforts to simulate core collapse supernova have not been able to provide a mechanism for robust explosions, several key features of the supernova dynamics and early evolution of the proto-neutron star are well understood. Large scale numerical simulations of supernova and neutron star evolution are now being pursued by several groups [1].

Simulating core collapse supernova is challenging because it involves coupled multi-dimensional hydrodynamics and neutrino transport. The neutrinos play a key role since they are the dominant source of energy transport. It is expected that refinements in neutrino transport and better treatment of multi-dimensional effects are needed to understand the explosion mechanism[1]. The temporal and spectral features of the neutrino

*This work is supported by the department of energy under contract w-7405-eng-36

emission which is emitted from the proto-neutron star is an independent diagnostic of supernova explosion dynamics and early evolution of the proto-neutron star. To accurately predict the ambient conditions just outside the newly born neutron star for the first $10 - 20$ s, we will need to understand both the explosion mechanism and neutrino emission. In this talk I will discuss micro-physical issues that directly affect the latter.

I begin by discussing the importance of the equation of state and neutrino transport in core collapse supernova in Sec. 2. Aspects of the equation of state and differences between predictions of mean field theories and variational calculations are discussed in Sec. 3. In Sec. 4, I discuss the micro-physics of neutrino opacity and its relation to linear response properties of dense matter. In Sec. 5, I conclude with a brief discussion of how neutrinos affect r-process nucleosynthesis.

2. Early Evolution of the Proto-Neutron Star

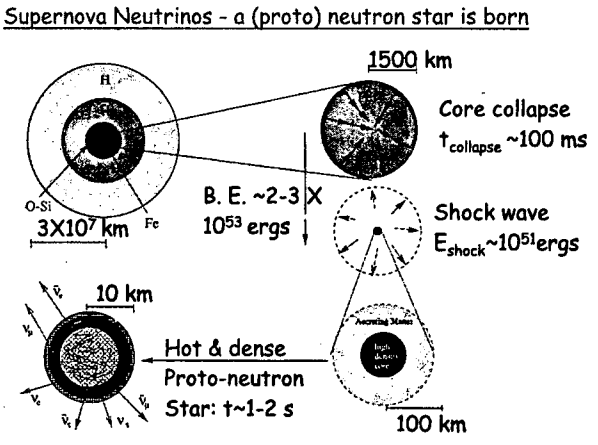

Figure 1. Schematic showing the various stages of a core-collapse supernova explosion.

The illustration in Fig.1, shows the important stages of core-collapse supernova and the birth of a proto-neutron stars. Successive nuclear burning from lighter to heavier elements, which fuels stellar evolution, inevitably results in the formation of a iron core in massive stars ($M \gtrsim 8M_{\odot}$). Since iron

is the most stable nucleus, further energy release through nuclear burning is not possible. The Fe-core is supported against gravitational collapse by the electron degeneracy pressure. When the mass of the Fe-core exceeds the Chandrashekar mass ($M_{\rm ch} \simeq 1.4 M_{\odot}$), it becomes unstable to gravitational collapse. Detailed numerical simulations indicate that the core collapses, from its initial radius $R_{\rm in} \simeq 1500$ km to a final radius $R_{\rm in} \simeq 100$ km, on a time-scale similar to the free-fall time-scale $\tau_{\rm free-fall} \simeq 100$ ms. Soon after the onset of collapse, the core density exceeds 10^{12} g/cm^3 and the matter temperature $T \simeq 5$ MeV. Under these conditions, thermal neutrinos become trapped on the dynamical time-scale of collapse. Consequently, collapse is nearly adiabatic. The enormous gravitational binding energy $B.E._{\rm Grav.} \simeq G M_{\rm NS}^2 / R_{\rm NS} \simeq 3 \times 10^{53}$ ergs, is stored inside the star as internal thermal energy of the matter components, and thermal and degeneracy energy of neutrinos. The newly born neutron star looses this energy on a time-scale determined by the rate of diffusion of neutrinos [2,3]. Neutrino

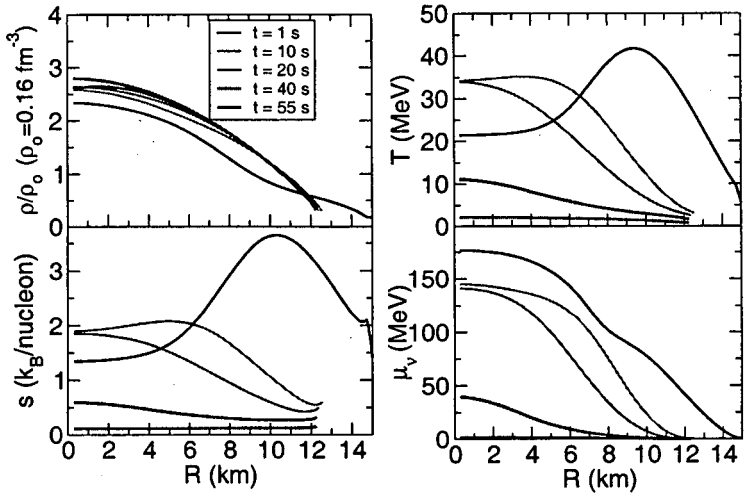

Figure 2. Snap shots of the proto-neutron star during its early evolution. Profiles of density, temperature, entropy and neutrino chemical potential are shown.

emission from the proto-neutron star has been studied within the diffusion approximation in earlier work [3]. Fig. 2 shows several time slices of the temperature, entropy per baryon, neutrino chemical potential and neutrino fraction inside the star as neutrinos diffuse radially outward. Initially, the

driving term for neutrino fluxes is the large gradient in the electron neutrino chemical potential (see figure). This phase of the evolution is called the deleptonization epoch. This epoch is characterized by joule-heating of the inner regions by the neutrino current driven by the lepton number gradient [2]. Subsequently, the neutrino fluxes are driven by the temperature gradient and results in cooling of the core. For this reason, this epoch is called the cooling phase. Time scales for deleptonization and cooling can be identified by inspecting the diffusion equations and are given by

$$\tau_D \simeq \frac{\partial Y_L}{\partial Y_\nu}\,\frac{R^2}{c\overline{\lambda}_e} \qquad \tau_C \simeq C_V\,\frac{R^2}{c\overline{\lambda}_\mu}\,, \tag{1}$$

respectively, where R is the radius of the proto-neutron star and c is the speed of neutrinos. In the above, $\overline{\lambda}_e$ is the typical mean free path of electron neutrinos which transport lepton number and $\overline{\lambda}_\mu$ is the mean free path of μ and τ neutrinos which transport energy. $\frac{\partial Y_L}{\partial Y_\nu}$ is related to the isospin susceptibility of nuclear matter (the symmetry energy) and C_V is the specific heat.

3. Nuclear Equation of State

The nuclear equation of state affects several aspects of the dynamics of core-collapse supernova. It directly affects the density and temperature profile to proto-neutron star and the location and energy of the shock wave. Here I will highlight some recent findings regarding the equation of state of neutron matter at sub nuclear density and identify generic differences between mean-field theoretic models for the EoS and the more microscopic variational calculations.

Although there are several models of the nuclear EoS, for the purpose of this discussion I shall broadly classify them into two categories: 1) mean field models (MFT) and 2) microscopic variational models. In the former, the starting point is an effective Lagrangian with a simplified form for the nucleon-nucleon interaction. The properties of nuclei or nuclear matter are calculated in the mean field approximation (typically only Hartree terms are retained) and are then used to fit the strength of the effective interactions. Fig. 3 shows a comparison between the EoS calculated in MFT and the microscopic model due to Akmal, Pandharipande and Ravenhall [4]. The mean field results are based on the Walecka model, but the trends seen are generic to large class of nuclear mean field predictions. We see that compared to microscopic calculations, the mean field EoS is stiff (higher pressure at the same energy density) at low density and soft (lower pressure

at the same energy density) at high density. While the high density behavior

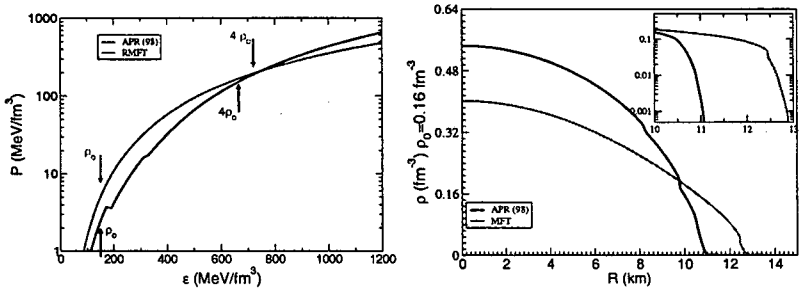

Figure 3. Comparison between mean field and microscopic equations of state. The resulting differences in the corresponding structure of a 1.4 $M_\odot$ neutron star is shown in the right panel.

is fairly uncertain in both approaches, we should expect the non-relativistic microscopic theories to provide a better description at low density. This is because they are derived from two-nucleon potentials that are obtained from nucleon-nucleon scattering data and the variational methods provide very detailed description of light nuclei. Further, at low density the large s-wave nucleon-nucleon scattering length (a_s) must dominate the interaction contribution to the equation of state. On general grounds, $a_s \to \infty$, we can expect the energy per particle to scale as $E_{\rm int} = \alpha\ E_{\rm FG}$ where $E_{\rm FG}$ is the energy per particle of a Fermi gas- there are no dimension full parameters in the low density limit and α must be a number. Microscopic calculations of neutron matter show similar behavior and predict that $\alpha \simeq 0.5$ while the low density of the mean field models with s-wave interactions predict a different behavior. Intriguingly, microscopic calculations seem to indicate that this behavior persists even when the inter-particle distance become comparable to the range of nuclear interaction[5].

4. Neutrino Interactions in Nucleonic Matter

It was realized over a decade ago that the effects due to degeneracy and strong interactions significantly alter the neutrino mean free paths and neutrino emissivities in dense matter [6,7], it is only recently that detailed calculations have become available [8,9,10,11]. The scattering and absorption

reactions that contribute to the neutrino opacity are

$$\nu_e + n \rightarrow e^- + p, \qquad \bar{\nu}_e + p \rightarrow e^+ + n,$$
$$\nu_X + A \rightarrow \nu_X + A, \qquad \nu_X + n(p) \rightarrow \nu_X + n(p), \qquad \nu_X + e^- \rightarrow \nu_X + e^-,$$

where $n, p, e^{\pm}, A$ represent neutrons, protons, positrons, electrons and heavy Fe-like nuclei, respectively. At low temperature ($T \lesssim 3-5$ MeV) and relatively low density ($\rho \simeq 10^{12} - 10^{13}$ g/cm^3, heavy nuclei are present and dominate the neutrino opacity due to coherent scattering. When the density is higher, $\rho \simeq 10^{13} - 10^{14}$ g/cm^3, novel heterogeneous phases of matter, called the "pasta" phases have been predicted to occur, where nuclei become extended and deformed progressively from spherical to rod-like and slab-like configurations[12]. For densities greater than 10^{14} g/cm^3, matter is expected to be a homogenous nuclear liquid. In what follows, we discuss the neutrino opacity in these different physical settings.

$\rho \simeq 10^{12}$ g/cm^3: At low temperature ($T \lesssim 5$ MeV), matter at these densities comprises of heavy nuclei (fully ionized), nucleons and degenerate electrons. The typical inter-particle distance, $d \simeq 20-40$fm. At these large distances, the nuclear force is small and the correlations between particles is dominated by the coulomb interaction. Since nuclei carry a large charge ($Z \simeq 25$) , the coulomb force between nuclei $F_{\rm Coulomb} \cong Z^2e^2/d$ dominates the non-ideal behavior of the plasma. Further, for low energy neutrinos which couple coherently to the total weak charge Q_W $25-40$ of the nucleus, neutrino scattering off nuclei is far more important than processes involving free nucleons and electrons [13].

The elastic cross-section for low energy coherent scattering off a nucleus (A,Z) with weak charge $Q_W = A - Z + Z\sin^2\theta_W$, where θ_W is the weak mixing angle, is given by[13]

$$\frac{d\sigma}{d\cos\theta} = \frac{1}{16\pi}\, G_{\rm F}^2\, Q_W^2\, E_\nu^2\, (1+\cos\theta) \tag{2}$$

When neutrinos scattering off nuclei in a plasma we must properly account for the presence of other nuclei since scattering from these different sources can interfere. In the language of many-body theory, this screening is encoded in the density-density correlation function [6,7]. The cross section for scattering of a neutrino with energy transfer ω and momentum transfer $\vec{q}$ is given by

$$\frac{d\sigma}{V\, d\omega\, d\cos\theta} = \frac{G_{\rm F}^2}{16\pi}\, Q_W^2\, (1+\cos\theta)\, S(|\vec{q}|,\omega) \tag{3}$$

$$\text{where} \qquad S(|\vec{q}|,\omega) = \frac{1}{2\pi\, N}\int dt\, \exp(i\omega t)\langle \rho(\vec{q},t)\rho(-\vec{q},0)\rangle\,. \tag{4}$$

The function $S(|\vec{q}|,\omega)$ is called the dynamic structure function and embodies all spatial and temporal correlations between target particles arising from strong or electromagnetic interactions. For a classical system of point

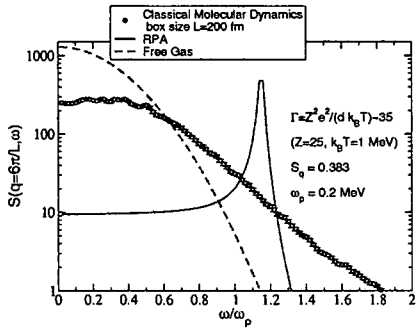

Figure 4. Dynamic structure function of a plasma of ions interacting as a function of energy transfer ω (measured in units of the plasma frequency $\omega_p = 0.2$ MeV) and fixed momentum transfer $|\vec{q}| = 6\pi/L = 18.6$ MeV.

particles interacting via a 2-body potential it is possible to simulate the real system using the methods of molecular dynamics (MD). Such numerical simulations confine N particles to a box with periodic boundary conditions and calculate the force on each particle at any time and evolve the particles by using their equations of motion. For $T \gtrsim 1$ MeV, the De-Broglie wavelength $\Lambda_D \ll d$ so the ionic gas is classical and we can use MD to calculate $S(|\vec{q}|,\omega)$. Fig.4 , shows the results of such a calculation. We chose to simulate 54 ions (A=50,Z=25) in a box of length $L = 200$ fm. For the classical simulations, a single, dimensionless, quantity $\Gamma = Z^2e^2/(4\pi d\ kT)$ characterizes the system. For $kT = 1$ MeV, $\Gamma \simeq 35$ for our system, corresponding to a strongly coupled plasma. The results in Fig.4 show a comparison between results obtained by MD simulations (dots with error bars) , free (Boltzmann) gas response (dashed-line) and response obtained using Random Phase Approximation (RPA). In RPA, Coulomb interactions are accounted for by selective re-summation of bubble graphs involving free excitations which interact via the Coulomb interaction. In particular, RPA is able to correctly predict the presence of well defined collective mode, corresponding to a phonon in the weak coupling regime ($\Gamma \lesssim 1$) and is often expected to provide a fair description of the long-wavelength response of correlated systems. However, as the comparison in Fig.4 indicates, both

RPA and the free gas response do poorly compared to MD. MD is exact in the classical limit and corrections to the classical evolution are small and expected to scale as λ_D/d. These results clearly illustrate that correlations can greatly affect the shape of the response and that approximate many-body methods such as RPA can fail when the coupling is strong, even at long-wavelengths.

$\rho \simeq 10^{13}$ g/cm^3: With increasing density, the nuclei get bigger and the inter-nuclear distance become smaller. Under these conditions, the nuclear surface and coulomb contributions to the Free energy of the system become important. It becomes energetically favorable for nuclei to become very deformed and assume novel, non-spherical, shapes such as rods and slabs [12]. Further, the energy differences between these various shapes are small $\Delta E \simeq 10 - 100$ keV. The dynamics of such an exotic heterogeneous phase is a complex problem involving several scales and forces. For temperatures of interest, $T \lesssim 5$ MeV, the De-Broglie wavelength and the inter-particle distance are comparable and quantum effects cannot be neglected. Recently, there have been attempts to model the behavior of these pasta phases using quantum molecular dynamics[15] and also find rod and slab like configurations.

How does the heterogeneity and existence of several low energy excitations involving shape fluctuations influence the response of this phase to neutrinos ? In the simplest description, the structure size (r) and the inter-structure (R) distance characterize the system. We can expect that neutrinos with wavelength large compared to the structure size but small compared to the inter-structure distance can couple coherently to the total weak charge (excess) of the structure, much like the coherence we discussed in the previous section. The effects of this coherent enhancement in the neutrino cross-sections has recently been investigated [16]. In agreement with our naive expectation, this study finds that the neutrino cross sections are enhanced by as much as an order of magnitude for neutrinos with energy $1/r \gtrsim E_\nu \gtrsim 1/R$.

$\rho \simeq 10^{14}$ g/cm^3: With increasing density, the novel structures discussed previously merge to form a homogeneous liquid of neutrons, protons and electrons. The response of such a Fermi-liquid has been investigated by several authors[8,10,11]. The general expression for the differential cross section

for the reaction $\nu_1 + 2 \rightarrow \nu_3 + 4$ is

$$\frac{1}{V}\frac{d^3\sigma}{d^2\Omega_3 dE_3} = -\frac{G_F^2}{128\pi^2}\frac{E_3}{E_1}\left[1-\exp\left(\frac{-q_0-(\mu_2-\mu_4)}{T}\right)\right]^{-1} \times (1-f_3(E_3))\ \mathrm{Im}\ \ (L^{\alpha\beta}\Pi^R_{\alpha\beta}), \quad (5)$$

where the incoming neutrino energy is E_1 and the outgoing electron energy is E_3, 2 is the initial state of the target particle and 4 is its final state[8,10]. The factor $[1-\exp((-q_0-\mu_2+\mu_4)/T)]^{-1}$ maintains detailed balance, for particles labeled '2' and '4' which are in thermal equilibrium at temperature T and in chemical equilibrium with chemical potentials μ_2 and μ_4, respectively. The final state blocking of the outgoing lepton is accounted for by the Pauli blocking factor $(1-f_3(E_3))$. The lepton tensor $L_{\alpha\beta}$and the target particle retarded polarization tensor $\Pi_{\alpha\beta}$ may be found in Ref. [10].

To account for the effects of strong and electromagnetic correlations between target neutrons, protons and electrons we must find ways to improve $\Pi_{\alpha,\beta}$. This involves improving the Greens functions for the particles and the associated vertex corrections that modify the current operators. In strongly coupled systems, these improvements are notoriously difficult and no exact analytic methods exist. One usually resorts to using mean-field theory to improve the Greens functions. Dressing the single particle Greens functions must be accompanied by corresponding corrections to the neutrino – dressed-particle vertex function. The random-phase approximation (RPA) can be thought of as such a vertex correction. Model calculations indicate that neutrino mean free paths computed in RPA tend to be a factor 2-3 times larger than in the uncorrelated system[10]. This is primarily because of repulsive forces in the spin-isospin channel, that suppress the axial response at low energies.

5. Discussion

Despite decades of work on supernova, the immediate vicinity of the proto-neutron star and the neutrino fluxes at early times are not well understood theoretically. In addition to macroscopic issues, the role of microphysics in the hydro and neutrino transport is only now being explored systematically. The physics issues discussed in this article, I hope have provided an overview of the current status. Both the EoS and neutrino opacities are sensitive to strong and electromagnetic corrections. Mean field theories and approximate many body methods such as RPA for response functions my provide qualitative guidance but more microscopic efforts are need for

quantitative predictions. These quantitative predictions for the neutrino luminosity and energy spectrum is important for the r-process since it affects both the entropy and the neutron-proton ratio of the neutron star wind [17].

Acknowledgments

I would like to thank Joe Carlson, Chuck Horowitz, Jim Lattimer, Jose Pons, Madappa Prakash for enjoyable collaborations and/or useful discussions. This work is supported in part by funds provided by the U.S. Department of Energy (D.O.E.) under the D.O.E. contract W-7405-ENG-36.

References

1. R. Buras, et al., Phys. Rev, Lett. **90**, 241101 (2003); A. Mezzacappa et al., Phys. Rev. Lett. **86**, 1935 (2001); Burrows, et al., Astrophys. J. **539**, 865 (2000)
2. A. Burrows, J.M. Lattimer: Astrophys. J. **307**, 178 (1986)
3. J. A. Pons, S. Reddy, M. Prakash, J. M. Lattimer and J. A. Miralles, Astrophys. J. **513**, 780 (1999).
4. A. Akmal, V. R. Pandharipande and D. G. Ravenhall, Phys. Rev. C **58**, 1804 (1998).
5. J. Carlson, J. . J. Morales, V. R. Pandharipande and D. G. Ravenhall, Phys. Rev. C **68**, 025802 (2003).
6. R. F. Sawyer, Phys. Rev. D **11**, 2740 (1975).
7. N. Iwamoto and C. J. Pethick, Phys. Rev. D **25**, 313 (1982).
8. C.J. Horowitz, K. Wehrberger: Nucl. Phys. A **531**, (1991) 665 ; Phys. Rev. Lett. **66**, 272 (1991); Phys. Lett. B **226**, 236 (1992)
9. G. Raffelt, D. Seckel: Phys. Rev. D **52**, 1780 (1995)
10. S. Reddy, M. Prakash, J.M. Lattimer: Phys. Rev. D **58**, 013009 (1998); S. Reddy, M. Prakash, J.M. Lattimer, J.A. Pons: Phys. Rev. C **59**, 2888 (1999)
11. A. Burrows, R.F. Sawyer: Phys: Rev. C **58**, 554 (1998); A. Burrows, R.F. Sawyer: Phys. Rev. C **59**, 510 (1999)
12. D. G. Ravenhall, C. J. Pethick and J. R. Wilson, Phys. Rev. Lett. **50**, 2066 (1983).
13. D. Z. Freedman, Phys. Rev. D **9**, 1389 (1974).
14. J.-P. Hansen, I. R. McDonald and E. L. Pollock, Phys. Rev. D **11**, 1025 (1975)
15. G. Watanabe, K. Sato, K. Yasuoka and T. Ebisuzaki, Phys. Rev. C **68**, 035806 (2003)
16. C. J. Horowitz, M. A. Perez-Garcia and J. Piekarewicz, arXiv:astro-ph/0401079.
17. Y. Z. Qian, Prog. Part. Nucl. Phys. **50**, 153 (2003).